Larhyss Journal, ISSN 1112-3680, n°53, Mars 2023, pp. 7-19

STRUCTURAL AND PHOTOCATALYTIC PROPERTIES OF NICKEL OXIDE (NIO) AND STANNIC OXIDE (SNO_2) NANOPARTICLES SYNTHESIZED VIA SOLVOTHERMAL PROCESS

ANANDAN K.[1]*, RAJESH K.[1], GAYATHRI K.[1], MOHANBABU M.[2], PRABHAKAR RAO P.[3]

[1.] Department of Physics, AMET University, Kanathur, Chennai, 603 112, India
[2.] Department of Physics, Sri Malolan College of Arts and Science, Madhurantakam, Kanchipuram, 603 306, India
[3.] Materials Science and Technology Division, National Institute for Interdisciplinary Science and Technology (NIIST), Thiruvananthapuram, 695 019 India

(*) anand.ka@ametuniv.ac.in

Research Article – Available at http://larhyss.net/ojs/index.php/larhyss/index
Received November 2, 2022, Received in revised form March 4, 2023, Accepted March 6, 2023

ABSTRACT

This work aims to study the structural and photocatalytic performance of p-type (NiO) and n-type (SnO_2) semiconductor metal oxides via the same synthesis process and conditions. The structural properties of the synthesized nickel oxide and stannic oxide nanoparticles were determined by X-ray diffraction. FTIR spectroscopy revealed the stretching vibration modes of Ni-O and Sn-O bonds. The performances of the NiO and SnO_2 nanoparticles in the photocatalytic degradation of methyl orange (MeO) dye under UV light were evaluated, and the degradation percentages (%) were found to be 63.63 and 88%; the detailed mechanism of the photocatalytic process and results were comparatively discussed.

Keywords: Semiconductors, Metal oxides, Nanoparticles, Solvothermal process, Structural properties, Photocatalytic activity

INTRODUCTION

Water pollution due to inorganic and organic pollutants has become a very sensitive issue worldwide. In recent years, water pollution caused by organic and toxic pollutants has attracted great attention. The sustained pollution of water by various organic and metallic ion contaminants has been the most serious, and many efforts have been devoted to the

remediation of environmental pollution. Nanomaterials are mainly used to overcome major water and wastewater problems. Nanoparticles are commonly used in the treatment of wastewater. Since nanoparticles have a large area and small sizes, they possess a strong adsorption reactivity and capacity. Metal oxide nanoparticles play a significant role in many areas (Naseem and Durrani, 2021; Ehtisham Khan et al., 2022; Qumar et al., 2022; Kasinathan et al., 2017; Krishnan et al., 2017), especially in wastewater treatments. In today's state-of-the-art materials, the facet, size, and shape of the synthesis of metal nanoparticles have significant importance (Adnan Younis et al., 2018; Chandra Purohit et al., 2021; Kokate et al., 2018; Arora, 2018; Sandhya and Ravichandra Babu, 2018; Basumatary and Changmai, 2018; Manglik and Singh, 2021). Photocatalysis has received much attention in recent times as a promising environmental remediation technique because of its ability to completely remove organic and inorganic toxins from water pollutants by using nanosized metal oxides as catalysts. To provide wholesome remediation, nanotechnology is a potential approach, focusing on unique attributes of materials emerging from nanoscale dimensions that ensure the purification of water resources. This is possible through photocatalysis, a property exhibited by semiconducting oxides or, more precisely, transition metal oxides (TMOs), whereby they absorb photons to undergo redox reactions, breaking complex organic molecules into simpler fragments. The diffusion length of charged carriers (e^-/h^+) from the bulk to the surface is significantly reduced for nanoparticles, facilitating the migration rate of these carriers and hence enhancing the photoactivity. Among a variety of transition metal oxides, nickel oxide (NiO) and stannic oxide (SnO_2) have received extensive attention as well-known p-type and n-type semiconducting materials with wide band gaps of 3.7 and 3.6 eV at room temperature, respectively (Akbari et al., 2020; Wana et al., 2013; Kasinathan et al., 2020; Godlaveeti et al., 2022). The successful utilization of such metal oxide nanomaterials in adsorption and photocatalysis is due to their large surface area, good pollutant loading capacity, specific affinity for various contaminants, and fast kinetics. As photocatalysts, metal oxide nanoparticles are used to degrade nondecomposed contaminants from water and wastewater (Dontsova et al., 2019). Among the methods, the solvothermal method has attracted much attention for its significant advantages, such as process scalability, the possibility of using different solvents, and easy control of the size and morphology of the product. Hence, it is quite promising and easy to use for industrial applications.

MATERIAL AND METHODS

Material and experimental procedure

All the chemical reagents used in our experiments were of analytical grade and were used as received without further purification. Cubic phase NiO and tetragonal structure SnO_2 nanoparticles were successfully synthesized by dissolving 0.441 g of nickel acetate tetrahydrate ($Ni(CH_3COO)_2.4H_2O$) and 0.876 g of tin chloride pentahydrate ($SnCl_4.5H_2O$) in 80 mL of ethanol in separate beakers. After a few minutes of vigorous

stirring, the solution was poured into a stainless steel autoclave. The solvothermal treatment was performed by placing the autoclave in an oven at 180°C for 24 hrs and naturally cooling it to room temperature. The light greenish and pale yellowish precipitates were collected and washed with distilled water and absolute ethanol by centrifugation several times to remove impurities. The final products were dried at 60°C for 5 hours under vacuum.

Characterization Techniques

The crystalline structure and size of the products were analyzed by using X-ray diffraction (XRD) with a JSO-Debyflex 2002 diffractometer (CuKα1 radiation (λ = 0.154 nm, 40 kV, 100 mA)). The chemical structure information of the nanoparticles (as pellets in KBr) was collected by FT-IR spectroscopy (Nicolet 205 spectrometer). The photocatalytic activities of the synthesized NiO and SnO_2 nanoparticles for the degradation of methyl orange (MeO) dye solution were investigated under ultraviolet (UV) light irradiation. The photocatalytic activity experiment was performed at room temperature.

Photocatalytic Experiment

Methyl orange (MeO), a well-known acid-base indicator, was chosen as a simple model of a series of common dyes largely used in the textile industry. The general characteristics of methyl orange dye are given below:

Chemical formula	$C_{14}H_{14}N_3NaO_3S$
Chemical structure	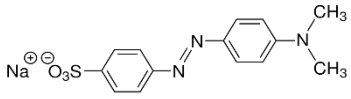
Molar mass	327.33 g/mol
Appearance	In an acidic medium, MeO is red In a basic medium, MeO is yellow.
pKa	3.4
pH range	3.1 – 4.4
Density	1.28 g/cm^3
Type	Anionic
Solubility	5 g/L (20°C)
Odor	Odorless

A photocatalytic experiment was carried out to investigate the photodegradation of methyl orange as a model organic compound. UV–Vis absorption spectra were obtained on a Perkin Elmer UV–Vis spectrometer (RX-1) using water as a solvent in the reference model. By adding 50 mg of the photocatalyst into 100 mL methyl orange (MeO) solutions, the photocatalytic degradation study was carried out using a 16 W UV lamp with a wavelength of 254 nm.

A graphical abstract of the synthesis process and characterization studies of NiO and SnO_2 nanoparticles is shown in Scheme 1.

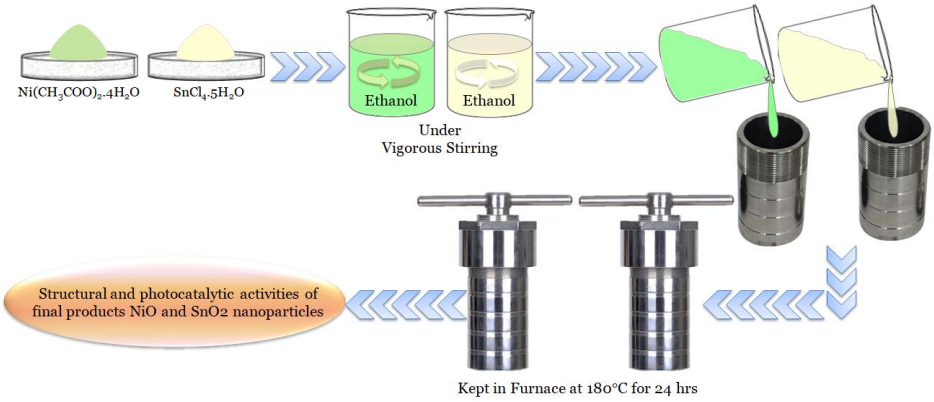

Scheme 1: Graphical abstract of synthesized NiO and SnO_2 nanoparticles and their characterization studies

RESULTS AND DISCUSSION

The structural properties of the synthesized nickel oxide and stannic oxide samples were analyzed. Fig. 1 shows the XRD patterns of the as-prepared NiO and SnO_2 nanoparticles, indicating the presence of a cubic phase of NiO and a tetragonal structure of SnO_2, which matched well with the standard data of nickel oxide (JCPDS card no.04-0835) and stannic oxide (JCPDS card no.41-1445), respectively (Hayat et al., 2011; Kasinathan and Varadarajan, 2015). There are no diffraction peaks from other impurities observed in the XRD patterns, from which it can be concluded that pure cubic phase NiO and tetragonal phase SnO_2 crystals were synthesized. The crystallite sizes of the samples were calculated by employing Debye-Scherrer's equation: $D = K\lambda/\beta\cos\theta$, where θ is the angle between the incident and diffracted beams (degree), β is the full with half maximum (rad.), D is the crystallite size of the sample (nm) and λ is the wavelength of the X-ray. The average crystallite sizes of the NiO and SnO_2 nanoparticles were calculated to be 18.56 and 6.21 nm, respectively.

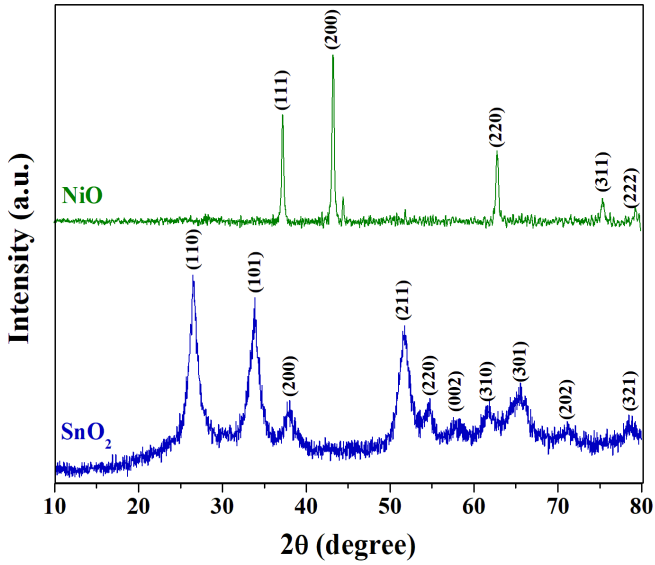

Figure 1: XRD patterns of NiO and SnO_2 nanoparticles

FTIR spectroscopy is a useful tool to investigate and understand the functional group of any organic molecule. The FTIR spectra of NiO and SnO_2 nanoparticles are shown in Fig. 2. Generally, the FTIR spectrum of metal oxides shows absorption bands below 1000 cm^{-1} due to their interatomic vibrations. The wide and shape bands at 3402 and 1624 cm^{-1} for NiO and 3424 and 1638 cm^{-1} for SnO_2 nanoparticles are mainly associated with the stretching and bending vibration modes of the O-H group on the surface of the products. The C_2H_5-O vibration of ethanol showed weak bands at 1036 and 1079 cm^{-1} for NiO and SnO_2 nanoparticles, respectively (Plyler, 1952). The broad absorption band at approximately 663 cm^{-1} in the NiO spectrum (in the range of 857– 412 cm^{-1}) is assigned to the Ni-O stretching vibration mode, and the broad absorption in the region of 792 – 491 cm^{-1} in the SnO_2 spectrum is attributed to the Sn-O stretching modes of Sn-O-Sn; the broadness of the absorption band indicates that the NiO and SnO_2 powders are well crystallized and nanocrystals (Ganachari et al., 2012; Song and kang, 2000). There was no evidence of a free precursor, nickel acetate, in the samples because the stretching vibrations of C=O ($\upsilon_{c=o}$) and C-O ($\upsilon_{c=o}$) disappeared. Therefore, the FTIR results agreed well with the XRD results.

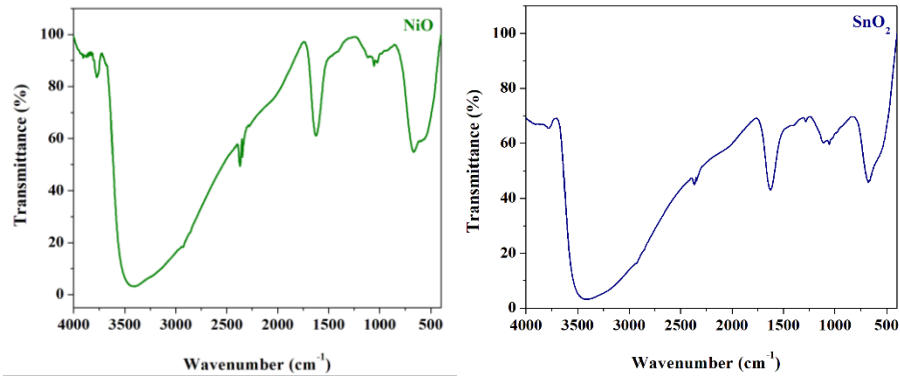

Figure 2: FTIR spectra of NiO and SnO_2 nanoparticles

The specific surface areas of the synthesized nickel oxide and stannic oxide nanoparticles were mathematically calculated by using $S = 6 \times 10^3 / d\rho$, where S, d, and ρ are the specific surface area, average crystallite size and density of the nickel oxide (6.67 g/cm^3) and stannic oxide (6.95 g/cm^3), respectively. The mathematically calculated surface areas of NiO and SnO_2 nanoparticles are 48.46 and 139.01 m^2g^{-1}, respectively, in which SnO_2 nanoparticles show greater surface area due to their smaller crystallite size.

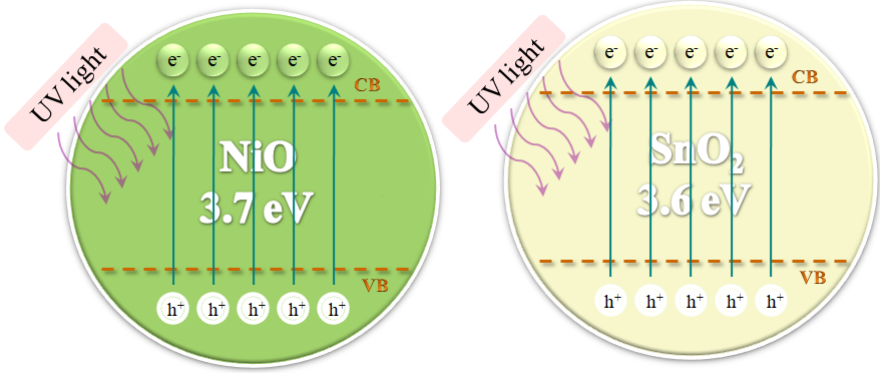

Scheme 2: Electron shifting from the valence to conduction band under UV light

With the same procedure, the two different types of semiconductor nanomaterials show different crystallite sizes, and the size effects of NiO and SnO_2 nanoparticles on photocatalytic activities were evaluated by the degradation of methyl orange (MeO) organic dye solution under UV light irradiation. UV–Vis spectra of aqueous MeO samples collected at various irradiation time intervals. From the absorption spectra, it was observed that as the irradiation time was increased up to 50 min in steps of 10 min, the absorbance at $ë_{max}$ = 463 nm gradually decreased. The photocatalytic efficiency was calculated using the relation $\eta = (1–C_r/C_0)$, where C_0 is the concentration of the dye before

illumination and C_r is the concentration of the dye after a certain irradiation time (Karimi et al., 2014).

To date, a variety of chemical and biological routes for removing colors from dye solutions have been proposed, but they can no longer be used due to their high cost, slow process, toxicity, high power consumption and creation of harmful byproducts. One of the most important advanced oxidation technologies is photocatalysis. It is commonly used for both oxidative and reductive wastewater treatment, such as the reductive deposition of metals from wastewater. Hence, the photocatalysis process appears to be an appropriate route for overcoming the constraints of such technologies. The fundamental benefit of photocatalytic degradation is that it eliminates the need for waste disposal because harmful contaminants are broken down into carbon dioxide, water, acid, and other simple salts. Valence and conduction bands are the pillars for the process of photocatalysis on the surface of metal oxide nanoparticles. UV light bombarding the NiO and SnO_2 nanomaterials generates electrons and transfers electrons from the valence band to the conduction band with corresponding energy higher than the band gap energy of the NiO and SnO_2 nanomaterials that should promote holes in the valence band and generate electrons in the conduction band (Narasaiah et al., 2022). Initially, under UV light irradiation, holes (h+) and electrons (e-) are generated in the valence and conduction bands on the surface of the metal oxide nanoparticles, respectively, which is represented in Scheme 2. Holes from the valence band and electrons from the conduction band play an important role in the process. Due to this action, oxidation and reduction processes occur and lead to the formation of high reactive oxygen species (ROS). This ROS is responsible for the degradation of methyl orange dye solution. These photogenerated pairs play an important role in the formation of highly aggressive radicals, i.e., hydroxyl ($\bullet OH^-$) and superoxide ($\bullet O_2^-$), from moisture and atmospheric oxygen. These radicals can oxidize and decompose organic materials and destroy bacteria (Andrade et al., 2017).

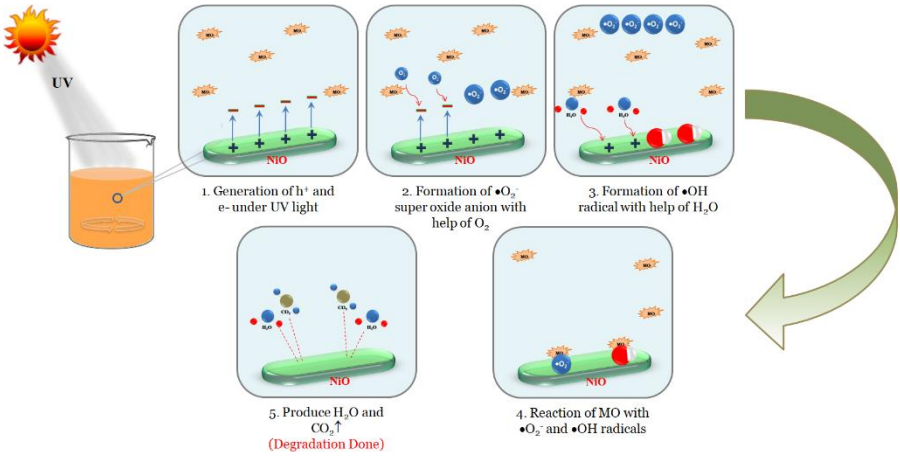

Scheme 3: Different stages of photodegradation of methyl orange solution under UV light as a NiO nanocatalyst

The possible mechanism involves sequence steps described by the following equations.

$NiO \text{ or } SnO_2 + h\nu \rightarrow (e^-)_{CB} + (h^+)_{VB}$

$(e^-)_{CB} + (h^+)_{VB} \rightarrow Heat$

$(e^-)_{CB} + O_2 \rightarrow \bullet O_2^-$

$\bullet O_2^- \rightarrow HO_2$

$2HO_2 \rightarrow O_2 + H_2O_2$

$H_2O_2 + \bullet O_2 \rightarrow \bullet OH + OH^- + O_2$

$(h^+)_{VB} + H_2O\ (OH^-) \rightarrow \bullet OH + H^+$

$\bullet OH \text{ or } \bullet O_2^- + MO\ (Dye) \rightarrow$ Intermediates $\rightarrow$ Degraded Products ($CO_2\uparrow + H_2O$)

From the schematic view of the photodegradation of methyl orange dye, which is shown in Scheme 3, in the very first step under UV irradiation, electrons and holes are formed in the conduction and valence bands, respectively. These photogenerated electron-hole pairs can either recombine or interact separately with other molecules. In the second step, the electrons present in the conduction band react with oxygen (O_2) to form superoxide radical anions ($\bullet O_2^-$), which help to produce a large number of hydroxyl radicals ($\bullet OH$), while in the third step, the positive holes (h^+) present in the valence band can react with moisture on the surface of the metal oxide nanoparticles or hydroxide ions to form highly reactive hydroxyl radicals ($\bullet OH$). In the fourth step, the highly reactive oxygen species (($\bullet OH$ and $\bullet O_2^-$) react with methyl orange dye molecules and decompose into CO_2 and H_2O in the final fifth step. The decomposition of methyl orange dye proceeds via oxidation by these $\bullet OH$ or $\bullet O_2^-$ radicals (Regraguy et al., 2022).

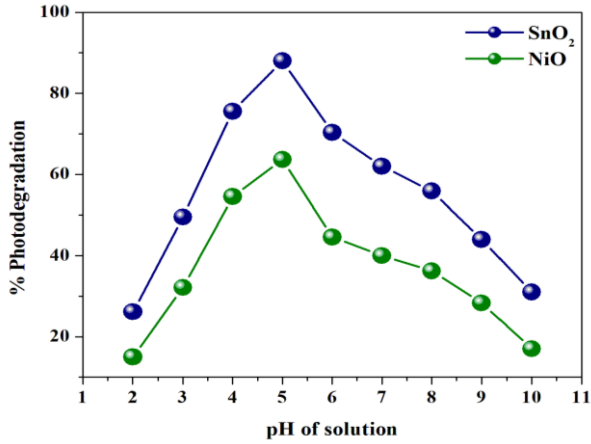

Figure 3: Photodegradation percentages of MeO dye solution as NiO and SnO_2 catalysts under different pH conditions.

Fig. 3 shows the effect of pH on the photodegradation percentage of NiO and SnO_2 nanocatalysts. The pH plays a starring role in the interaction between adsorbate and adsorbent owing to its impact on adsorbent surface properties and on the dissociation or ionization of adsorbate molecules. To determine the effect of pH on the photodegradation of the methyl orange dye solution by using NiO and SnO_2 nanoparticles as catalysts, the pH of the dye solution varied from 2 to 10 by using H_2SO_4 and NaOH with constant amounts of photocatalyst, concentration of dye solutions and irradiation time (50 min). Under these conditions, the results demonstrate that the adsorption capacity and percentage removal of MO dye increased gradually as the pH increased with respect to the UV irradiation time. This may be related to the amount of photogenerated electron–hole pairs that are produced due to the sensitization of photocatalyst nanoparticles. However, at pH 5, photodegradation was found to be maximum for nickel oxide and stannic oxide nanocatalysts. This result indicated that both metal oxide nanocatalysts under less acidic conditions are favorable for the construction of reactive intermediates, such as hydroxyl radicals, which are extensively improved, further enhancing the reaction rate.

Fig. 4 shows the degradation percentage of the MeO dye versus irradiation time intervals in the presence of nanocatalyst. The degradation percentages (%) of the MeO dye were calculated as 63.63 and 88 for the NiO and SnO_2 catalysts, respectively. Due to the smaller crystallite size and greater surface area-to-volume ratio of the SnO_2 catalyst, (Bushell et al., 2020) showed a higher degradation percentage. A comparison of the different parameters of the synthesized NiO and SnO_2 nanoparticles is listed in Table 1.

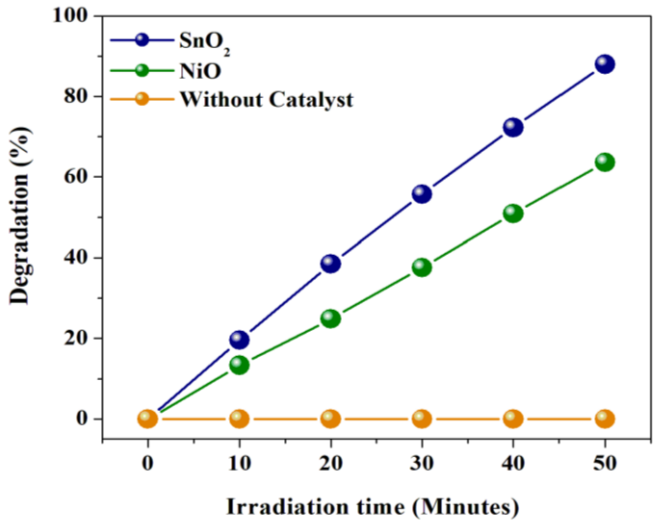

Figure 4: Degradation percentages of MeO dye solution with NiO and SnO_2 catalysts under UV illumination.

Table 1: Comparison of different parameters of synthesized NiO and SnO_2 nanoparticles.

Name of the Metal Oxide	Crystallite Size (nm)	Specific Surface Area - SSA (m^2g^{-1})	Photocatalytic Degradation (%)
NiO	18.56	48.46	63.63
SnO_2	6.21	139.01	88

CONCLUSION

P-type and n-type semiconductor metal oxides, such as nickel oxide (NiO) and stannic (SnO_2) nanoparticles, were synthesized via a simple solvothermal process under similar conditions. The structural properties and crystallite sizes of the synthesized nanoparticles were evaluated by X-ray diffraction and FTIR spectroscopy. The results show that NiO and SnO_2 have cubic and tetragonal structures, respectively. The photocatalytic performance of the nanoparticles was comparatively discussed. Both metal oxide nanocatalysts show maximum photodegration at pH 5. Stannic oxide shows better photocatalytic performance due to its smaller crystalline size and high surface-to-volume ratio. Hence, these metal oxide nanoparticles are promising materials in textile industries for wastewater cleaning.

Declaration of competing interest

The authors declare that they have no known competing financial interests or personal relationships that could have appeared to influence the work reported in this paper.

REFERENCES

ADNAN YOUNIS M., BUKHARI I.H., ABBAS Q., BIN TALIB N., SHAUKAT S. (2018). Synthesis, importance and applications of metal oxide nanomaterials, International Journal of Technology, Vol.8, Issue 2, pp. 49-57.

AKBARI A., SABOURI Z., HOSSEINI H. A., HASHEMZADEH A., KHATAMI M., DARROUDI M. (2020). Effect of nickel oxide nanoparticles as a photocatalyst in dyes degradation and evaluation of effective parameters in their removal from aqueous environments, Inorganic Chemistry Communications, Issue 115, Paper 107867.

ANDRADE G.R.S., NASCIMENTO C.C., LIMA Z.M., TEIXEIRA-NETO E., COSTA L.P., GIMENEZ I.F., (2017). Star-shaped ZnO/Ag hybrid nanostructures for enhanced photocatalysis and antibacterial activity, Applied Surface Science, Vol. 399, pp. 573-582.

ARORA A.K. (2018). Metal/Mixed Metal Oxides and Their Applications as Sensors: A Review, Asian Journal of Research Chemistry, Vol. 11, Issue 2, pp. 497-504.

BASUMATARY S., CHANGMAI N. (2018). Biological Materials Assisted Synthesis of Silver Nanoparticles and Potential Applications: A Review, Research Journal of Pharmacy and Technology, Vol. 11, Issue 6, pp. 2681-2694.

BUSHELL M., BEAUCHEMIN S., KUNC F., GARDNER D., OVENS J., TOLL F., KENNEDY D., NGUYEN K., VLADISAVLJEVIC D., RASMUSSEN P.E., JOHNSTON L.J. (2020). Characterization of Commercial Metal Oxide Nanomaterials: Crystalline Phase, Particle Size and Specific Surface Area, Nanomaterials, Vol. 10, Issue 9, pp. 1-19.

DONTSOVA T.A., NAHIRNIAK S.V., ASTRELIN I.M. (2019). Metaloxide Nanomaterials and Nanocomposites of Ecological Purpose, Journal of Nanomaterials, Vol. 2019, pp. 1-31.

EHTISHAM KHAN M., MOHAMMAD A., ALI W., AHMED SHARWANI A.R. (2022). Recent developments in properties and applications of metal oxides, Inorganic Anticorrosive Materials, Vol. 2022, pp. 95-111.

GANACHARI S.V., BHAT R., DESHPANDE R., ABBARAJU V. (2012). Synthesis and characterization of nickel oxide nanoparticles by self-propagating low temperature combustion method, Recent Research in Science and Technology, Vol. 4, Issue 4, pp. 50-53.

GODLAVEETI S.K., SOMALA A.R., SANA S.S., QULADSMANE M., GHFAR A., NAGIREDDY R.R. (2022). Evaluation of pH Effect of Tin Oxide (SnO_2) Nanoparticles on Photocatalytic Degradation, Dielectric and Supercapacitor Applications, Journal of Cluster Science, Vol. 33, pp. 1635–1644.

HAYAT K., GONDAL M.A., KHALED M.M., AHMED S. (2011). Effect of operational key parameters on photocatalytic degradation of phenol using nano nickel oxide synthesized by sol–gel method, Journal of Molecular Catalysis a Chemical, Vol. 336, Issue 1-2, pp. 64–71.

KARIMI L., ZOHOORI S., YAZDANSHENAS M.E. (2014). Photocatalytic degradation of azo dyes in aqueous solutions under UV irradiation using nano-strontium titanate as the nanophotocatalyst, Journal of Saudi Chemical Society, Vol. 18, Issue 5, pp. 581-588.

KASINATHAN A., KRISHNAN R., KRISHNAN, G., SELVARASU V.S., MOHAMMED HUSSAIN S.G., VARADARAJAN R. (2020). Effects of rare earth, transition and post transition metal ions on structural and optical properties and photocatalytic activities of zirconia (ZrO_2) nanoparticles synthesized via the facile precipitation process, Physica E: Low-dimensional Systems and Nanostructures, Vol. 124, Issue 10, pp. 114342.

KASINATHAN A., KRISHNAN R., VARADARAJAN R., (2017). Enhanced optical properties of spherical zirconia (ZrO_2) nanoparticles synthesized via the facile various solvents mediated solvothermal process, Journal of Materials Science: Materials in Electronics, Vol. 28, Issue 22, pp. 17321-17330.

KASINATHAN A., VARADARAJAN R., (2015). Influence of dopant concentrations (Mn = 1, 2 and 3 mol%) on the structural, magnetic and optical properties and photocatalytic activities of SnO_2 nanoparticles synthesized via the simple precipitation process, Superlattices and Microstructures, Vol. 85, Issue 9, pp. 185-197.

KOKATE K.K., KULKARNI S., BHANDARKAR S.E. (2018). Synthesis, Characterization of PEDOT-Metal Oxides Nanocomposites and use of PEDOT-ZnO nanocomposite as the Photoanode in Dye sensitized solar cells (DSSC), Asian Journal of Research Chemistry, Vol. 11, Issue 1, pp. 91-102.

KRISHNAN R., AYYANAR M., KASINATHAN A., POOVATHINGAL P.K., (2017). Crystal and optical perfection, linear and nonlinear optical quanlities of β alanine β alaninium picrate (βAβAP) single crystal: a promising NLO crystal for optics and photonics applications, Journal of Materials Science: Materials in Electronics, Vol. 28, Issue 15, pp. 11446 – 11454.

MANGLIK S., SINGH J. (2021). A Review on Nanoparticles: Preparation and Characterization of Nanoparticles, Research Journal of Topical and Cosmetic Sciences, Vol. 12, Issue 2, pp. 79-5.

NARASAIAH B.P., BANOTH P., SOHAN A., MANDAL B.K., DOMINGUEZ A.G.B., VALLADARES L.D.L.S., KOLLU P., (2022). Green Biosynthesis of Tin Oxide Nanomaterials Mediated by Agro Waste Cotton Boll Peel Extracts for the Remediation of Environmental Pollutant Dyes, ACS Omega, Vol. 7, Issue 18, pp. 15423–15438.

NASEEM T., DURRANI T. (2021). The role of some important metal oxide nanoparticles for wastewater and antibacterial applications, A review, Environmental Chemistry and Ecotoxicology, Vol. 3, pp. 59-75.

PLYLER E.K. (1952). Infrared Spectra of Methanol, Ethanol, and n-Propanol, Journal of Research of the National Bureau of Standards, Vol. 48, Issue 4, pp. 281-286.

PUROHIT M.C., KANDWAL A., PUROHIT R., SEMWAL A.R., PARVEEN S., KHAJURIA A.K. (2021). Antimicrobial Activity of Synthesized Zinc Oxide Nanoparticles using Ajuga bracteosa Leaf Extract, Asian Journal of Pharmaceutical Analysis, Vol. 11, Issue 4, pp. 275-280.

QUMAR U., HASSAN J.Z., BHATTI R.A., RAZA A., NAZIR G., NABGAN W., IKRAM M. (2022). Photocatalysis vs adsorption by metal oxide nanoparticles, Journal of Materials Science & Technology, Vol. 131, Issue 20, pp. 122-166.

REGRAGUY B., RAHMANI M., MABROUKI J., DRHIMER F., ELLOUZI I., MAHMOU C., ABDELMALEK D., EI MRABET M., EI HAJJAJI S., (2022). Photocatalytic degradation of methyl orange in the presence of nanoparticles $NiSO_4/TiO_2$ Nanotechnology for Environmental Engineering, Vol. 2, Issue 7, pp. 157-171.

SANDHYA G., RAVICHANDRA BABU R. (2018). Synthesis and Characterization Co and Mg Co-doped TiO_2 Nanoparticles, Asian Journal of Research Chemistry, Vol. 11, Issue 3, pp. 645-648.

SONG K.C., KANG Y. (2000). Preparation of high surface area tin oxide powders by a homogeneous precipitation method, Materials Letters, Vol. 42, Issue 5, pp. 283-289.

WANA X., YUANA M., TIEA S.L., LANB S. (2013). Effects of catalyst characters on the photocatalytic activity and process of NiO nanoparticles in the degradation of methylene blue, Applied Surface Science, Vol. 277, Issue 15, pp. 40-46.